

# A Novel Design of Non-Uniform Reflectarrays with Symbolic Regression and its Realization using 3-D Printer

Peyman Mahouti<sup>1</sup>, Filiz Güneş<sup>1</sup>, Mehmet A. Belen<sup>2</sup>, and Alper Çalışkan<sup>1</sup>

<sup>1</sup>Department of Electronics and Communication Engineering  
University of Yıldız Technical, Istanbul, TURKEY  
pmahouti@yildiz.edu.tr, gunes@yildiz.edu.tr, acaliskan@yildiz.edu.tr

<sup>2</sup>Department of Electric and Electronic Engineering  
University of Artvin Çoruh, Artvin, TURKEY  
mehmetlibelen@artvin.edu.tr

**Abstract** — Herein, a novel design of an X-band Non-Uniform Reflectarray Antenna (NURA) with Symbolic Regression SR and its fabrication using 3D Printer technology are presented. A NURA is consist of simply a grounded dielectric layer with the variable thickness. Firstly, SR is employed to obtain with a great accuracy for the reflection phase characteristics of a grounded dielectric layer in the analytical form within the continuous domain of  $1 \leq \epsilon_r \leq 6$  and thickness  $0.1 \leq h \leq 3$  mm for the X-band. For this purpose, SR is trained and validated by the 3D CST Microwave Studio data. Then, for the design purpose of NURA, a special fine reflection calibration characteristic is built up again by SR with the sufficient reflection phase range of the 3D Printer's material at the operation frequency 10 GHz. In the third step, the designed NURA is then prototyped by using 3D printer technology where the material can be easily shaped and create unit cell at printing accuracy of 0.1 mm per layer. Thus, by this mean the prototyping cost of non-uniform Reflectarray design can be reduced drastically both in means of time and ease of manufacturing. In the final step, mismatching and radiation properties of the prototyped NURA are measured.

**Index Terms** — 3D printer, antenna design, microstrip reflectarrays, reflection phase modelling, symbolic regression.

## I. INTRODUCTION

A Microstrip Reflectarray Antenna (MRA) is a design that being a hybrid of a reflector antenna and a planar phased array antenna which uses a suitable phasing scheme for its elements to reflect the incoming electromagnetic wave form a pencil beam in a specified direction  $(\theta^0, \varphi^0)$  [1-4]. One of the very popular phasing schemes involves varying dimensions of the elements such as printed dipoles or patches around their resonant

size. In the recent works of [3-4], novel multi-objective evolutionary design optimization procedures are put forward to obtain the quasilinear phasing characteristic for the Minkowski RA s using 3D CST Microwave Studio based Multilayer Perceptron Neural Network (MLP) models with Particle Swarm and hybrid Genetic Algorithm (GA) and Nelder-Mead (NM) algorithms, respectively. In fact, MRAs are advantageous antennas having the simple structures with low profiles, light weights and no need of any complicated feeding networks. However, MRA s are inherently narrow-band radiating elements and the mutual couplings between microstrip elements printed on standard substrates are significant; in addition, the conductor and surface wave loss are severe. To reduce these shortcomings solely grounded dielectric layer with variable thickness is proposed to be used as a reflecting surface in [5]. In this Non-Uniform dielectric layer, the required phase shift is provided by determining thickness at each cell on the RA plane to produce a pencil reflected beam in a specific direction  $(\theta^0, \varphi^0)$ . Thus, a RA design with the possible simpler and more advantageous structure can be obtained than MRAs.

In this work, a novel approach for design and fabrication of Non-uniform Reflectarray Antenna (NURA) had been proposed. Firstly in the design stage, SR [6] is applied to express the reflection phase characteristics of a grounded dielectric layer in the form of an analytical expression within the domain of  $1 \leq \epsilon_r \leq 6$  with variable thickness  $0.1 \leq h \leq 3$  mm using the 3-D EM based data sets for X-band (8-12 GHz) applications. Then, for the design purpose, a special fine calibration characteristic is built up by SR with the sufficient reflection phase range for the 3D Printer's material PLA with  $\epsilon_r=2.4$  at the operation frequency 10GHz. SR Eureqa is a novel regression method that performs genetic programming within the mathematical expression domain to create a model consisting of summation of

expressions that fits to a given dataset with a great accuracy [7-8]. This regression method nowadays has been used to obtain solutions for various science and engineering problems [9-12]. In the recent work [12], SR has been employed to uncover intrinsic relationships hidden within the Big Data that is derivation of a full-wave simulation based analytical expression for the characteristic impedance  $Z_0$  of microstrip lines. In [12], Big Data is obtained from the CST Microwave Studio, in terms of the substrate dielectric constant  $\epsilon$ , height  $h$  and strip width  $w$  within 1-10 GHz band.

Recently, 3-D printing technology has been used for the prototyping of microwave designs [13-22]. 3D printing method has many advantages compared with the traditional fabrication methods such as being easier to prototype complex designs in terms of low cost and low weight. Herein, 3D printer technology is used for prototyping of the designed NURA. One of the most recent innovation for fast and accurate prototyping is 3D printing technology.

The paper is organized as follows: The next section gives the basics of SR and application to the reflection calibration characteristics of NURA. In this section, for the purpose of training and validation, 3D CST data set is obtained for the substrates with dielectric permittivity ( $1 \leq \epsilon_r \leq 6$ ) and height ( $0.1 \text{ mm} \leq h \leq 3 \text{ mm}$ ) using the waveguide simulator is briefly explained and a continuous function fitted to this data set is built up using SR, finally validation will be given. The third section is devoted to the design of NURA using SR, which is made from the 3D Printer's material PLA with  $\epsilon_r=2.4$  at the operation frequency 10GHz, alongside of fabrication by 3D printer. Finally, the work ends with conclusions.

## II. SYMBOLIC REGRESSION AND APPLICATION TO NURA

Symbolic Regression (SR) is used to discover mathematical expressions of functions that can fit the given data based on the rules of accuracy, simplicity, and generalization. This method builds a model consisting of solely an accurate analytical expression formed recombining the ready base functions using some evolutionary algorithms such as Genetic Programming (GP) [6], Gene Expression Programming (GEP) [23], Grammatical Evolution (GE) [24], Analytic Programming (AP) [25], and some optimization problems [26-27]. The main advantage of SR is that it does not require any specific structure or parameter, instead reveals intrinsic relationships within the dataset letting its patterns. Thus this analytical model enables a designer a rapid optimization and analysis of the complicated electromagnetic devices instead using computationally inefficient commercial full wave simulators. In this work, SR in the design stage that is based on GP. Main principle of GP based SR is such that expressions (Eqs. 1-5) are represented in chromosomes like syntactic trees.

The syntactic tree form of Eq. (1) is given in Fig. 1 for a better understanding. Based on GA principles, new individuals (children) whose representations are in fact new expressions which are evaluated by fitness, are created either by random generators, or by exchanging parent's parts by crossover or mutation operators. As an example for SR regression process, the expression given in Eqs. (1-2) are taken as Parents and Eqs. (3-5) are the children of these parents through cross over or mutation operations:

$$P_1 = f(a, b, c, d, e) = \sin\left(\frac{ab}{c}\right) + \sqrt{d-e} + a^2, \quad (1)$$

$$P_2 = \cos(ab) - e^c + \sqrt{\frac{d}{e}}, \quad (2)$$

$$C_1 = \sin\left(\frac{ab}{c}\right) - e^c + a^2, \quad (3)$$

$$C_2 = \cos(ab) - e^c - 17e, \quad (4)$$

$$C_3 = \sin\left(\frac{ab}{c}\right) + (d-e)^2 + a^2. \quad (5)$$

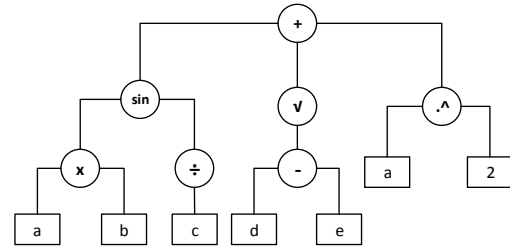


Fig. 1. An example of syntactic tree.

In Fig. 2, a typical NURA design is given in which with the variation of the height in the unit elements the reflection phase is changed and is focus on a desired direction.

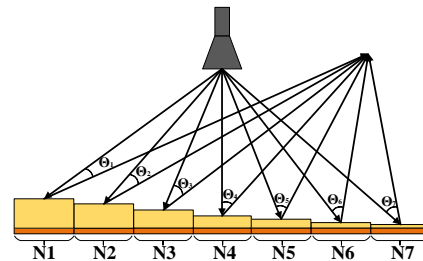


Fig. 2. Centre fed Non-Uniform Reflect Array.

The reflection phase characteristics of a grounded dielectric layer  $1 \leq \epsilon_r \leq 6$  with variable thickness  $0.1 \leq h \leq 3$  mm are obtained using the H-wall simulator [2] in order to form an analytical expression for X-band (8-12 GHz) applications. For this purpose, the required training and

validation data sets of reflection phase of unit cell given in Fig. 3 are generated by the 3-D EM simulation tool CST.

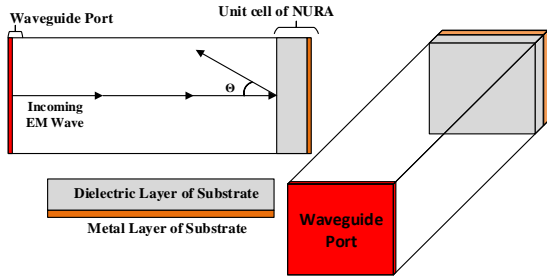


Fig. 3. Unit Cell of the NURA with its simulation setup.

The top and bottom surfaces of the H-wall waveguide simulator are perfectly electric conducting walls, while the right and left walls are perfectly magnetic field walls [2]. The vertically polarized incoming waves will be incident normally onto the element at the end of the waveguide at the broadside direction and then reflected back also at the broadside direction with a set of amplitude and phase information. A series of simulations are carried out to gather training and test data samples Tables 1 and 2 for SR search of Reflection Phase by using CST 3D EM simulation tool, respectively.

Table 1: Training data set for Reflection Phase expression

Parameter	Sample Ranges	Sample Step
<b>Dielectric Permittivity</b>	1-6	0.25
<b>Substrates Height (mm)</b>	0.3-3	0.1
<b>Frequency (GHz)</b>	8-12	0.5
<b>Total</b>	5292	

Table 2: Test data set for Reflection Phase expression

Rogers	$\epsilon_r$	Height (mm)	Frequency (GHz)	Total
<b>4003</b>	3.55	0.305, 0.406, 0.508 0.813, 1.524	8-12	12012
<b>4350</b>	3.66	0.338, 0.76, 1.52	8-12	
<b>5870</b>	2.33	0.127*, 0.381, 0.508, 0.787, 1.575 3.175*	8-12	

\*Values out of training dataset range.

The 5292 data in Table 1 are used as the training data in Eureqa environment [6] to perform SR search. The following commands are used to start the SR search:

- Use data points equally for training and validation purposes;

- Use all basic formula blocks;
- Use all exponential blocks;
- Use Mean Absolute Error as error-metric (Default).

Thus, the targeted analytical expression for Reflection Phase (RP) is obtained as a function of dielectric constant  $\epsilon_r$ , height  $h$ , frequency  $f$  as follows:

$$RP = 541.73 - \frac{3.1\epsilon_r^2 (hf)^2}{10^6} - \frac{0.5}{h} + \frac{0.62 + 0.019(hf)^2}{0.97 + \epsilon_r} - (45.59 + 2.68h) f. \quad (6)$$

The performance of the obtained expression is validated by Eureqa itself, however we also validated accuracy of the model using approximately 12,000 additionally test data belonging to the typical X-band substrates as given in Table 2, even we also tested extrapolation performance. In this analysis, the common error-metrics measures are employed which are Mean Absolute Error (MAE), Relative Mean Error (RME) and Maximum Error (MXE) as given in Eqs. (7-9) for both training and test data:

$$MAE = \frac{1}{N} \sum_{i=1}^N |T_i - P_i|, \quad (7)$$

$$RME = \frac{1}{N} \sum_{i=1}^N \frac{|T_i - P_i|}{|T_i|}, \quad (8)$$

$$MXE = \max(T_i - P_i). \quad (9)$$

Table 3: Performance of Analytical Expression

Error Metric (Degree)	Training Data	Test Data
<b>MAE</b>	0.27	0.1027
<b>RME</b>	0.0006	0.0003
<b>MXE</b>	13.96	0.3586

Results of the performance measures of Eq. (6) are presented at Table 3 alongside of Figs. 4-5 of reflection phase versus variable substrate height for typical  $\epsilon_r$ ,  $f$  values as compared with CST values.

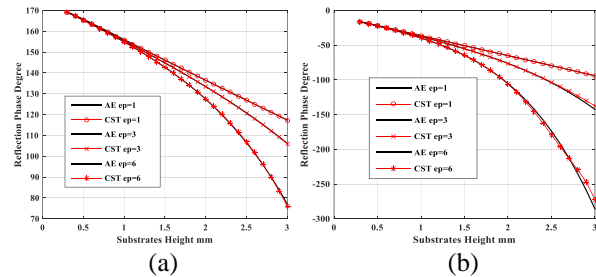


Fig. 4. Reflection Phase Characteristics for variable dielectric permittivity and height for: (a) 8 GHz and (b) 12 GHz.

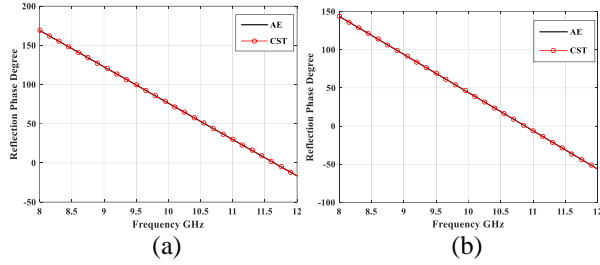


Fig. 5. Reflection Phase Characteristic for Rogers: (a) 4003 ( $h=0.305$ ,  $\epsilon_r=3.55$ ), and (b) 5870 ( $h=1.575$ ,  $\epsilon_r=2.33$ ).

### III. 3D FABRICATION AND EXPERIMENTAL WORK

Fast and accurate prototyping process of microwave devices and antennas have an extreme importance for design process. In today’s RF and microwave technology, there is an ever-increasing demand for higher level of fast, low cost and accurate prototyping. One of the most recent innovation for fast and accurate prototyping is 3D printing technology. 3D printing is a method of manufacturing in which materials, such as plastic or metal, are deposited onto one another in the form of layers to produce a three dimensional object, such as a pair of eye glasses or other 3D objects. To date, 3D printing has primarily been used in engineering to create engineering prototypes.

In this work, firstly the 3D model is exported in “.STL” file format, so that the CEL Robox® Micro [28] (Fig. 6) can create its code for printing of the prototype. Also, in case of large structure models, the model can be sliced into smaller parts, where in here, the prototyped antenna model given in Fig. 7 was sliced into smaller size parts (1/12). The material used for 3D printer is PLA “Black as Night” [29] with a dielectric constant of 2.4 and the printing accuracy (printed layer height) is chosen as 0.1 mm for the best quality printing results.

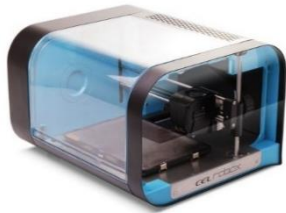


Fig. 6. CEL Robox® Micro manufacturing platform [28].

Applying the same process given in Section II, a new and simpler Reflection Calibration Characteristic having almost 360° phase range is obtained using SR Eureka with the 270 CST data in Table 4 where for the substrate height variation is taken between 0.5-10 mm

which is considered as 0.1 mm sample steps:

$$Phase = 1.88 + \frac{21.2}{h} - (0.022h^2 - 0.51h + 3.19)h^3 . \quad (10)$$

Table 4: Training data set for Limited Reflection Phase expression

Parameter	Sample Ranges	Sample Step
Substrate Height (mm)	0.5-10	0.1
Dielectric Permittivity	2.4	
Frequency (GHz)	10	
Total	270	

Since the NURA is symmetric with respect to the center, thus Table 5 gives heights of the quadratic NURA being divided 10 segments and starting from the corner point. The values given in Table 5, are necessary compensation values at each element using the Eq. (10) to convert spherical wave to the plane wave [1]. Thus, a pencil beam in the normal direction of the RA plane, is achieved by designing the height of each RA cell using the Reflection Phase Calibration Characteristic in Fig. 8, to reflect the incident wave independently with a phase compensation proportional to the distance from the phase centre of the feed-horn as well-known from the classical array theory [1].



Fig. 7. Prototyped 3D printed NURA.

Table 5: Parameter values of quadratic NURA in (mm)

ID	1	2	3	4	5	6	7	8	9	10
1	1.7	1.7	1.7	2.8	3.9	5	6.3	8.7	2.4	4.4
2	1.7	1.7	2.2	3.2	4.1	5.2	6.6	9.2	2.7	4.7
3	1.7	2.2	2.9	3.7	4.6	5.7	7.3	1.7	3.3	5.1
4	2.8	3.2	3.7	4.5	5.3	6.5	8.6	1.9	4	5.7
5	3.9	4.1	4.6	5.3	6.3	7.8	1.7	3.2	4.8	6.7
6	5	5.2	5.7	6.5	7.8	1.7	2.8	4.3	5.9	8.3
7	6.3	6.6	7.3	8.6	1.7	2.8	4.2	5.5	7.3	1.7
8	8.7	9.2	1.7	1.9	3.2	4.3	5.5	7.1	1.7	3.2
9	2.4	2.7	3.3	4	4.8	5.9	7.3	1.7	3.1	4.8
10	4.4	4.7	5.1	5.7	6.7	8.3	1.7	3.2	4.8	6.4

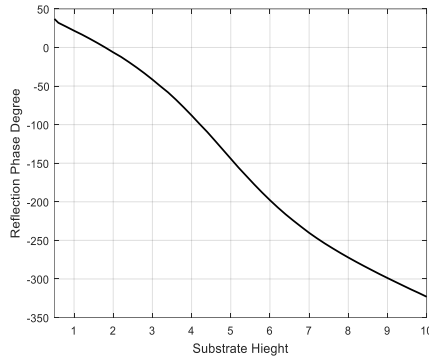


Fig. 8. Reflection phase calibration characteristic of material with dielectric permittivity of 2.4 at 10 GHz.

In Figs 9-10, the measurement results of the prototyped NURA design are presented. As it can be observed from the measurement results, the VSWR characteristics of the NURA is below 2 in all X band. Also, the design has a gain of almost 22dB at 10 GHz. The gain measurement results of NURA, show a 1 dB gain bandwidth of almost the 21% and confirm the promising characteristics of such radiating element. The feed is prime focus, positioned with an  $F/D = 0.66$ .

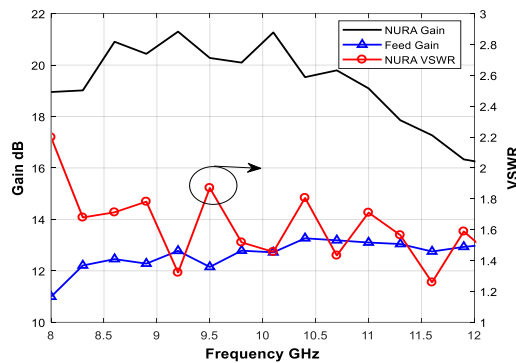


Fig. 9. Measured NURA Characteristics Gain-VSWR, over Frequency band.

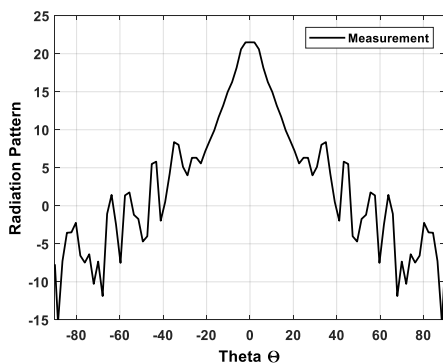


Fig. 10. Measured Far Field Gain performance of NURA at 10 GHz.

## IV. CONCLUSION

In this work, a novel regression SR and prototyping method which is 3D printing is applied to the realization of the Non-Uniform Reflect-Array (NURA). As it can be seen from the results, SR is used as a successful tool for building an accurate analytical expression for the reflection phase calibration characteristic of NURA that is used in a fast design optimization and performance analysis. The required amount of training data is comparable with the counterpart regression methods [12], in spite of this, a model consisting of a solely single analytical expression is resulted revealing the intrinsic relationships of the data set using the existing data patterns. Therefore, this method can be efficiently employed in the accurate, fast modelling and design optimization of electromagnetic devices in the form of analytical expressions. The training and test data is also share publicly in [30].

In the realization step, the designed NURA is prototyped by using 3D printer technology where the PLA material can be easily shaped and create unit cell at printing accuracy of 0.1 mm per layer. Thus, by this mean the prototyping cost of NURA design can be reduced drastically both in means of time and ease of manufacturing. Measurements of the mismatching and radiation properties of the realized NURA are resulted to be agreed with the novel theoretical performances.

## ACKNOWLEDGEMENT

We would like to express our special thanks of gratitude to the Research Fund of the Yildiz Technical University for founding our research under project number FAP-2018-3427, TÜBİTAK 2211/A, to Aktif Nesor Elektronik, and Nutonian, Inc. for providing researcher's licenses for our use.

## REFERENCES

- [1] D. M. Pozar and T. A. Metzler, "Analysis of a reflect array antenna using microstrip patches of variable size," *Electronics Letters*, vol. 27, pp. 657-658, 1993.
- [2] J. Huang and J. A. Encinar, *Reflect Array Antennas*. Wiley-IEEE Press, ISBN: 978-0470-08491-4, 2007.
- [3] F. Güneş, S. Nesil, and S. Demirel, "Design and analysis of Minkowski reflectarray antenna using 3-D CST Microwave Studio-based neural network model with particle swarm optimization," *International Journal of RF and Microwave Computer-Aided Engineering*, vol. 23, no. 2, pp. 272-284, Mar. 2013. (DOI: 10.1002/mmce.20711).
- [4] F. Güneş, S. Demirel, and S. Nesil, "A novel design approach to X-band Minkowski reflectarray antennas using the full-wave EM simulation-based complete neural model with a hybrid GA-NM algorithm," *Radioengineering*, vol. 23, no. 1, Apr. 2014.
- [5] M. Moeini-Fard and M. Khalaj-Amirhosseini, "Non-

- uniform reflect-array antennas,” *Int. J. RF and Microwave Comp. Aid. Eng.*, vol. 22, pp. 575-580, 2012.
- [6] Eureka 1.24.0 (2015). Available: <http://www.nutonian.com/products/eureka/demo/contact/>
- [7] J. R. Koza, *Genetic Programming*. MIT Press, ISBN 0-262-11189-6, 1998.
- [8] J. R. Koza, F. H. Bennet, D. Andre, and M. Keane, *Genetic Programming III*. Morgan Kaufmann Pub., ISBN 1-55860-543-6, 1999.
- [9] M. Schmidt and M. Lipson, “Distilling free-form natural laws from experimental data,” *Science*, vol. 324, no. 5923, pp. 81-85, 2009.
- [10] V. Ceperic, N. Bako, and A. Baric, “A symbolic regression-based modelling strategy of AC/DC rectifiers for RFID applications,” *Expert Systems with Applications*, vol. 41, iss. 16, pp. 7061-7067, 2014.
- [11] M. M. Hasan, A. Sharma, F. Johnson, G. Mariethoz, and A. Seed, “Correcting bias in radar Z-R relationships due to uncertainty in point rain gauge networks,” *Journal of Hydrology*, 2014. DOI: <http://dx.doi.org/10.1016/j.jhydrol.2014.09.060>
- [12] P. Mahouti, F. Güneş, M. A. Belen, and S. Demirel, “Symbolic regression for derivation of an accurate analytical formulation using “big data”: An application example,” *ACES Journal*, vol. 32, no. 5, May 2017.
- [13] P. Nayeri, M. Liang, R. A. Sabory-Garcia, M. Tuo, F. Yang, M. Gehm, H. Xin, and A. Z. Elsherbeni, “3D printed dielectric reflectarrays: Low-cost high-gain antennas at submillimeter waves,” *IEEE Trans. Antennas Propag.*, vol. 62, no. 4, pp. 2000-2008, Apr. 2014.
- [14] J.-M. Floch, B. El Jaafari, and A. El Sayed Ahmed, “New compact broadband GSM/UMTS/LTE antenna realized by 3D printing,” *The 9th European Conference on Antennas and Propagation*, Lisbon, Portugal, Apr. 2015.
- [15] A. G. Lopez, E. L. C. Ernesto, R. Chandra, and A. J. Johansson, “Optimization and fabrication by 3D printing of a volcano smoke antenna for UWB applications,” *7th European Conference on Antennas and Propagation (EuCAP)*, pp. 1471-1473, Apr. 2013.
- [16] M. Mirzaee, S. Noghianian, and Y. Chang, “Low-profile bowtie antenna with 3D printed substrate,” *Microw. Opt. Technol. Lett.*, vol. 59, pp. 706-710, 2017.
- [17] M. Ahmadloo and P. Mousavi, “Application of novel integrated dielectric and conductive ink 3D printing technique for fabrication of conical spiral antennas,” *IEEE Antennas and Propagation Society International Symposium (APSURSI)*, pp. 780-781, July 2013.
- [18] M. Mirzaee, S. Noghianian, L. Wiest, and Y. Chang, “Developing flexible 3D printed antenna using conductive ABS materials,” *IEEE International Symposium on Antenna and Propagation and North American Radio Science Meeting 2015*, pp. 1308-1309, July 2015.
- [19] B. Y. Ahn, E. B. Duoss, M. J. Motala, X. Guo, S.-I. Park, Y. Xiong, J. Yoon, R. G. Nuzzo, J. A. Rogers, and J. A. Lewis, “Omnidirectional printing of flexible, stretchable, and spanning silver micro-electrodes,” *Science*, vol. 323, no. 5921, pp. 1590-1593, Mar. 2009.
- [20] J. J. Adams, S. C. Slimmer, J. A. Lewis, and J. T. Bernhard, “3D-printed spherical dipole antenna integrated on small RF node,” *Electron. Lett.*, vol. 51, no. 9, pp. 661-662, Apr. 2015.
- [21] M. A. Belen and P. Mahouti, “Design and realization of quasi Yagi antenna for indoor application with 3D printing technology,” *Microw Opt Technol Lett.*, 60 (9), pp. 2177-2181, 2018. <https://doi.org/10.1002/mop.31319>
- [22] Y. C. Toy, P. Mahouti, F. Güneş, and M. A. Belen, “Design and Manufacturing of an X-Band Horn Antenna using 3-D Printing Technology,” *8th International Conference on Recent Advances in Space Technologies*, İstanbul, Turkey, 19-22 June 2017.
- [23] C. Ferreira, “Gene expression programming: a new adaptive algorithm for solving problems,” *Complex Systems*, vol. 13, no. 2, pp. 87-129, 2001.
- [24] M. O'Neill and C. Ryan, “Grammatical evolution,” *IEEE Transactions on Evolutionary Computation*, vol. 5, no. 4, pp. 349-358, 2001.
- [25] Z. Oplatkova and I. Zelinka, “Symbolic regression and evolutionary computation in setting an optimal trajectory for a robot,” in *Proceedings of the 18th International Workshop on Database and Expert Systems Applications (DEXA '07)*, IEEE, Regensburg, Germany, pp. 168-172, Sep. 2007.
- [26] Y. Rahmat-Samii and E. Michielssen, *Electromagnetic Optimization by Genetic Algorithms*. John Wiley & Sons, Inc., 1999.
- [27] J. M. Jeevani W. Jayasinghe, J. Anguera, D. N. Uduwawala, and A. Andújar, “Nonuniform overlapping method in designing microstrip patch antennas using genetic algorithm optimization,” *International Journal of Antennas and Propagation*, vol. 2015.
- [28] Robox by CEL – A micro manufacturing platform, <https://www.cel-uk.com/shop/robox-by-cel-a-micro-manufacturing-platform-with-dual-nozzle-fff-head-rbx01/> [23.03.2019].
- [29] PLA Filament “Black as Night,” Model Number RBX-PLA-BK092.
- [30] P. Mahouti, M. Ali Belen, A. Çalışkan, and F. Güneş, “Phase characterization of the nonuniform reflect arrays,” *IEEE Dataport*, 2018. [Online]. Available: <http://dx.doi.org/10.21227/H2BW8F>. Accessed: May 28, 2018.